

ORIGINAL ARTICLE

Novel glycidyl methacrylated dextran/gelatin nanoparticles loaded with basic fibroblast growth factor: formulation and characteristics

Chunhu Gu¹, Renhong Zheng², Zhifu Yang³, Aidong Wen³, Hong Wu⁴, Hui Zhang⁴ and Dinghua Yi¹

¹Department of Cardiovascular Surgery, Xijing Hospital, Fourth Military Medical University, Xi'an, China, ²Department of Hepato-Biliary Surgery, Xijing Hospital, Fourth Military Medical University, Xi'an, China, ³Department of Pharmacy, Xijing Hospital, Fourth Military Medical University, Xi'an, China and ⁴Department of Pharmaceutics, Fourth Military Medical University, Xi'an, China

Abstract

Objective: To develop a novel efficient nanoparticulate carrier loaded with basic fibroblast growth factor (bFGF). **Methods:** Gelatin and glycidyl methacrylate-derivatized dextran (dex-GMA) were cross-linked and polymerized to form interpenetrating polymeric networks. The properties of the nanoparticles (NPs) were investigated as a function of the degree of dex-GMA substitution and the concentration of gelatin used in the preparation of the hydrogels. The morphology was observed with scanning electron microscopy and transmission electron microscopy. The swelling, degradation, and entrapment efficiency were also determined by dynamic evaluation methods in vitro. The protein release ratio and in vitro release kinetics were evaluated by routine procedure, and the biological activity of bFGF-loaded NPs was studied by cell proliferation assay, cell attachment, and cell function. **Results:** The NPs have a particle size of 320 ± 20 nm. bFGF was entrapped in the nanoparticles quantitatively (the encapsulation efficiency, $89.6 \pm 0.9\%$). The bFGF in vitro release kinetics fitted to zero-order and Higuchi equations. Proliferation assay, attachment assay, and western blot showed that bFGF NPs had good biological effects on cultured bone marrow mesenchymal stem cells and could achieve a much longer action time than bFGF solution. **Conclusion:** These results suggested that a novel biodegradable dex-GMA/gelatin hydrogel NPs loaded with bFGF could be successfully developed from both dextran- and gelatin-based biomaterials.

Key words: Basic fibrous growth factor; dextran; drug delivery system; gelatin; nanoparticle

Introduction

The growth and differentiation factors, extracellular matrix proteins, and adhesive factors have been widely utilized in wound healing and in regenerative area and tissue engineering^{1–3}. However, the lack of suitable methods for delivering the appropriate dose of growth factors to the objective tissue is an obstacle to the clinical application. Because of the rapid clearance and relatively short biological half-life of these proteins, direct administration of the human recombinant growth factor proteins is not effective. Repeated injections or use

of the growth factors would consequently be necessary, which is neither clinically acceptable nor economical. For these drugs to be used therapeutically or economically, suitable drug delivery systems such as locally controlled delivery devices that are capable of encapsulating and providing sustained release of bioactive proteins are desirable.

Encapsulating proteins into different types of biomaterials is the most common method of fabricating a controlled delivery device. Recently, a number of organic or inorganic, natural or artificial materials have been developed for drug delivery in experimental or

Chunhu Gu, Zhifu Yang and Renhong Zheng are co-first authors.

Address for correspondence: Dr. Dinghua Yi, Department of Cardiovascular Surgery, Xijing Hospital, Fourth Military Medical University, 15th Changle West Road, Xi'an 710032, China. Tel: +86 29 84775311, Fax: +86 29 83210092. E-mail: guchunhu@fmmu.edu.cn

Dr. Hong Wu, Department of Pharmaceutics, Fourth Military Medical University, 17th Changle West Road, Xi'an 710032, China. E-mail: wuhxa@yahoo.com.cn

(Received 17 Aug 2008; accepted 21 Apr 2009)

preclinical models⁴⁻⁸. Dextran has attracted much more attention for use in a controlled drug delivery system because of its excellent hydrophilic nature and biocompatibility⁹. Dextran is a hydrophilic natural polysaccharide consisting of mainly $\alpha(1\rightarrow6)$ -linked D-glucose units and three hydroxyl functional groups per anhydroglucose residue and is versatile for chemical modification as well as for network formation¹⁰. The characteristic α -1,6-glucosidic linkage is hydrolyzed by dextranases, enzymes produced by various molds, and certain bacteria as well as by mammalian cells. So, it is susceptible to enzymatic digestion in the body. Frequently, for improved biocompatibility and release, investigated oxide-hydroxide-modified cross-linked dextran is glycidyl methacrylated dextran (dex-GMA), which could be synthesized by coupling GMAs to those hydroxyl functional groups of dextran by an experimental method adapted from van Dijk-Wolthuis et al.¹¹

Previous studies carried out by our group^{12,13} have demonstrated that locally controlled release of insulin-like growth factor-I (IGF-I) had good function with the locally controlled release from dextran-co-gelatin hydrogel microspheres. The hydrogel microspheres had a particle size of $32 \pm 2 \mu\text{m}$. During the initial stages, the microspheres sopped up and the sphere enlarged, and the drug was rapidly released from microspheres through the exoteric microaperture. When the swelling was counterpoise, the drug release would slow down and be determined by drug pervasion and microsphere biodegradation. The drug release profile fitted in vitro to first-order manner and Higuchi equation had an initial burst release. Moreover, the drug had a relatively short release period. Therefore, to meet more wide biomedical use in pharmaceutical and biopharmaceutical fields in vivo and in vitro, designing to control drug release rate over an extended duration or at a specific time during treatment, minimizing drug burst release, and significantly diminishing the particles size to widen the application area are of great importance in the drug delivery system.

In recent years, significant effort has been taken to develop nanotechnologies for drug delivery¹⁴. Nanoparticles (NPs) have been used to provide localized delivery of biomolecules to targeted tissues, to solubilize drugs for intravascular delivery, and to improve the stability of therapeutic agents, especially peptides, proteins, and nucleic acid drugs, against enzymatic degradation. The nanometer size ranges of these delivery systems can offer certain distinct advantages for drug delivery in tissue engineering and regenerative medicine. Because of their submicrometer size, NPs have demonstrated relatively greater intracellular uptake than microparticles¹⁵. This permits efficient delivery of therapeutic agents to target sites in the body¹⁶. Additionally, the release of a therapeutic agent from NPs could be controlled by modulating polymer characteristics to

achieve desired therapeutic levels in target tissue for a duration sufficient for optimal therapeutic efficiency^{17,18}. Furthermore, NPs can be delivered to distant target tissues either by localized delivery by a catheter-based approach with a minimally invasive procedure or by conjugation to a biospecific ligand, which can direct them to the target tissue^{16,17}.

Taking all these factors into consideration, we recently developed a polymeric dex-GMA/gelatin NPs incorporating basic fibroblast growth factor (bFGF) using a method adapted from Kosmala et al.¹⁹ with modification^{14,20,21}. Our dex-GMA/gelatin NPs system has been developed with the aim of (i) making an ideal delivery system that is suitable for intravenous administration and (ii) obtaining sustaining drug release as long as possible at the local site. This work mainly described the synthesis, physicochemical properties, and biological effects of the novel nanoparticulate protein carrier in vitro.

Materials and methods

Dextran T-40 was purchased from Xiasi Chemical Co. (Beijing, China). Acidic gelatin with isoelectric point (IEP) 9.0 (Mw 100 kDa) was supplied by NittaGelatin Co. (Osaka, Japan); GMAs, ammonium persulfate (APS), and *N,N,N',N'*-tetramethylethylenediamine (TEMED) were obtained from Amresco (Solon, OH, USA). bFGF was a product of Sigma Systems (Sigma Aldrich, St. Louis, MO, USA), in the form of an aqueous solution (IEP 9.6). Enzyme-linked immunoadsorption assay (ELISA) kit was purchased from Invitrogen Systems (Invitrogen, Carlsbad, CA, USA). All other chemicals and organic solvents were purchased at their highest purity from Sigma Aldrich.

Preparation of the dextran-glycidyl methacrylate

Glycidyl dex-GMA with different degree of substitution (DS: the number of GMA molecules per 100 glucose moieties) were synthesized by coupling GMA to dextran by a method adapted from van Dijk-Wolthuis et al.¹¹ with alterations^{12,13}. Briefly, dextran (5 g) was dissolved in dimethyl sulfoxide (DMSO) solvent (50 mL) under nitrogen atmosphere. After dissolution of 4-dimethylamino-pyridine (1 g), a calculated amount of GMA was then added at a very slow rate. The solution was stirred at room temperature for 48 hours, after which the reaction was stopped by adding an equimolar amount of concentrated HCl to neutralize the 4-dimethylamino-pyridine. The reaction solution was recrystallized with dehydrated alcohol (200 mL). After vacuum filtration for separating dex-GMA and DMSO, the resulting white precipitate was dissolved in distilled water (10 mL) at 4°C. Subsequently, the solution was extensively dialyzed against distilled water by dialysis membrane tubing

having a molecular weight cutoff of 12 kD (Sigma Diagnostic Inc., Orlando, FL, USA) at 4°C for 72 hours with refreshment of distilled water every 12 hours. dex-GMA was lyophilized, and the white fluffy product was stored at 4°C before use. The degree of GMA substitution was determined to be 4.3% and 6.7% by ^1H nuclear magnetic resonance (NMR).

Preparation of NPs

Interpenetrating polymeric networks (IPNs) can be formed from dex-GMA cross-linked in the presence of gelatin. Taking the score of appearance and the size distribution as bases, we studied the influence of the concentration of gelatin and dex-GMA on the performance of these NPs. Several other factors, such as APS concentration and curing time, were found to have less influence on those properties of the beads. Therefore, these factors were kept constant throughout this study. A two-factor, three-level Box-Behnken design or the optimization process by a statistical software (Statgraphics Plus, version 4.1; Manugistics Inc., Rockville, MD, USA) was used. The best preparation method of the NPs was optimized, and the finished products were given an initial determination, namely 20 wt.% dex-GMA and gelatin. In short, aqueous solutions of dex-GMA and gelatin in 0.22 M APS (50 mg/mL) were flushed for 10 minutes with N_2 gas and subsequently transferred into a scintillation vial. The best preparation method of the NPs was optimized. Aqueous solutions of dex-GMA (20%, w/w) and gelatin of 5% in 0.22 M APS were flushed for 10 minutes with N_2 gas and subsequently transferred into paraffin liquid (50 mL). The two-phase system was vigorously mixed (vortex, type Scientific Industries, Vortex Genie 2, Model G-560-E, maximum intensity) for 60 seconds to create a water-in-water emulsion by adding Span-80 (180 μL , 50 mg/mL). Next, the emulsion was followed by the addition of TEMED (10 μL , 20%, v/v) at room temperature. This system was incubated for 2 hours at 37°C to polymerize the methacryloyl groups coupled to the dex-GMA chains. The collected NPs were hardened with 1% glycerinaldehydes for 24 hours, which was followed by freeze-drying. Using different (DS, 4.3 and 6.7) dex-GMA, two types of dex-GMA/gelatin hydrogel NPs (NPs with DS 4.3 and NPs with DS 6.7, each type consisted of three samples differing in the concentration of gelatin) were synthesized in this study.

The bFGF-loaded NPs were prepared by the same procedure. bFGF-loaded dex-GMA/gelatin hydrogels were prepared by the polymerization of an aqueous solution of dex-GMA, mixture of the protein bFGF (concentration 5 $\mu\text{g}/\text{mL}$), and acidic gelatin (IEP 9.0)²¹ in phosphate-buffered saline (PBS, 0.2 M, pH 7.4) as the methods previously described²². The polymerization was initiated by APS (concentration 50 mg/mL) and

TEMED (final concentration 60 $\mu\text{mol}/\text{g}$). The reaction mixture was polymerized in lagena for 1 hour. The temperature increased because the liberated polymerization heat was marginal (<0.5°C), thereby excluding thermal denaturation of the entrapped proteins. This solution volume was below the nanoparticle's theoretical equilibrium swelling volume to allow for complete drug absorption. The resulting mixture was vortexed and incubated at 4°C for 15 hours before freeze-drying. The configurations of freeze-dried NPs were also examined.

Nanoparticle characterization

Nanoparticle size and size distribution

The average nanoparticle size and morphology were examined by an S-2700 transmission electron microscope (Hitachi, Tokyo, Japan) at a voltage of 80 kV. One drop of NPs was placed on copper grids and negatively stained with 2% phosphotungstic acid for 30 seconds. The aqueous dispersion of the particles was drop-cast onto a carbon-coated copper grid. The particle size was determined by a laser diffraction particles size analyzer (Shimadzu SALD 1100). The freeze-dried nanoparticle morphology was examined under a scanning electron microscope (JEOL 840A, Tokyo, Japan) at an accelerating voltage of 5 kV and a working distance of 8.0 or 8.2 mm.

Swelling and degradation of dex-GMA/gelatin hydrogel NPs

To examine the behaviors of hydrogel NPs based on dex-GMA, we determined the swelling ratios (SRs) and degradation properties at 37°C in the presence of dextranase. Dried dex-GMA/gelatin hydrogel NPs, accurately weighed (W_i), were immersed in PBS (10 mM, pH 7.4) in an orbital shaker at 120 rpm at 37°C for 24 hours to equilibrate to fully hydrated state and weighed to obtain a wet weight. At different time intervals, the swollen hydrogel NPs were removed and washed thrice with distilled water and centrifuged thrice, blotted dry, and lyophilized on a freeze drier for 24 hours. The dry hydrogel at different time intervals was accurately weighed (W_t). After W_t determination, either SR or mass remaining rate was calculated from the following equation:

$$\text{SR } (\%, w/w) = \frac{(W_s - W_t)}{W_t} \times 100\%$$

$$\text{Mass remaining rate } (\%, w/w) = \frac{W_t}{W_i} \times 100\%,$$

where W_s is the weight of the swollen hydrogel NPs, W_i is the weight of dried hydrogel NPs before test, and W_t is the weight of dried hydrogel NPs at time of t .

Entrapment efficiency of dex-GMA/gelatin hydrogel NPs

The percentage value of the loaded bFGF (% bFGF loaded) was calculated as follows: first, the amount of drug associated with NPs was calculated as the difference between the total amount of bFGF added to the system called bFGF_t (theoretic) and the bFGF recovered in the supernatant (bFGF_s) assuming that the bFGF not recovered in the supernatant was encapsulated in the NPs. Subsequently, the ratio between bFGF encapsulated in NPs and the mass of NPs (NPs) was calculated and expressed as percentage (% bFGF loaded) according to the following equation:

$$\% \text{ bFGF loaded} = \frac{(\text{bFGF}_t - \text{bFGF}_s)}{\text{NPs}} \times 100\%.$$

The entrapment efficiency of bFGF was described as (bFGF_t minus; bFGF_s)/bFGF_t × 100%; bFGF remaining in the supernatant was determined with ELISA kit (Invitrogen Systems).

In vitro release kinetic study of dex-GMA/gelatin hydrogel NPs

The kinetics of bFGF release from NPs with different DS and different concentration of gelatin was determined in PBS absent or present dextranase (final enzyme concentration 0.15 U/mL). Each sample was immersed in 5-mL microcentrifuge tubes containing 3.5 mL of PBS (pH 7.4) and 0.02% (w/v) sodium azide. The samples were incubated at 37°C under continuous agitation. After 2, 4, 8, 16, 24 hours, 4, 8, 12, 16, 20, 24, 28, 32, and 40 days, the supernatant of each specimen was collected. The amounts of bFGF in the supernatants were determined with ELISA kit (Invitrogen). The experiments were performed in quintet. The percentage of bFGF released was determined from the following equation: release (%) = [bFGF]_{ft}/[bFGF]_T × 100%, where [bFGF]_{ft} is the concentration of bFGF in the filtrate at time *t* and [bFGF]_T is the total amount of bFGF entrapped in the NPs.

Bioactivity of bFGF-loaded dex-GMA/gelatin hydrogel NPs

Isolation and culture of bone marrow mesenchymal stem cells from mouse

Mesenchymal stem cells (MSCs) from bone marrow of Sprague–Dawley mouse were isolated and cultured by a method described by Kopen et al.²³ The cells were determined by fluorescence-activating cell sorting (Beckman Coulter, Fullerton, CA, USA) analysis before the experiments by directly conjugated antibodies against anti-mouse CD44 [fluorescein isothiocyanate conjugate (FITC); Invitrogen], anti-CD29 (FITC; Caltag,

San Francisco, CA, USA), anti-CD45 (FITC; Invitrogen), and anti-CD90 (FITC; Invitrogen). The cells between passage 3 and passage 5 were used.

Cell proliferation assay

Sprague–Dawley mouse bone marrow MSCs (BMSCs) were detached from the culture flasks by trypsin–EDTA, and the cell suspension was adjusted at 5×10^4 cells/mL in culture medium. One hundred microliters of this cell suspension containing 5×10^3 cells was seeded in each well of a 96-well tissue culture plate (GIBCO Life Technologies, Karlsruhe, Germany). Cells were cultivated in the DMEM containing 4500 mg/L D-glucose, 100 IU/mL penicillin, 100 g/mL streptomycin, 50 µg/mL ascorbic acid, and 10% FCS in the absence (control) or presence of 10 ng/mL bFGF and 1 mg/mL bFGF-loaded NPs (dex-GMA/gelatin hydrogel NPs, equal to 10 ng/mL bFGF) at 37°C in humidified air containing 5% CO₂ for 2, 3, 5, 7, and 10 days. After being cultured, the metabolic cell activity was measured by tetrazolium salt assay. Cells were incubated for 4 hours with tetrazolium salt [3-(4,5-dimethylthiazol-2-yl)-2,5-diphenyl-2,5-tetrazolium bromide (MTT), final concentration 0.5 mg/mL] at 37°C. Formed formazan crystals were solubilized, and the absorbance was measured at 540 nm wavelength by a microtiter plate reader (Titertek, Helsinki, Finland).

Cell attachment

Cell attachment was measured by a modified colorimetric method according to Landegren²⁴ with some modifications. Briefly, passage 3 cells were detached from tissue culture flasks with a 0.05% trypsin/0.1% EDTA solution. The cells were subsequently washed in serum-free media. Then the bone MSCs were re-seeded onto 60-mm dishes at a density of 1×10^5 cells per dish and allowed to attach for different times (3, 6, and 24 hours) in the DMEM containing 10% FCS in the absence (control) or presence of 10 ng/mL bFGF and 1 mg/mL bFGF-loaded NPs (dex-GMA/gelatin hydrogel NPs, equal to 10 ng/mL bFGF) at 37°C in humidified air containing 5% CO₂. Then, nonadherent cells were removed by washings with 0.1 M PBS (pH 7.4). Chromogenic substrate solution of 500 µL [7.5 mM substrate (*p*-nitrophenyl *N*-acetyl β-D glucosaminide); 0.1 M Na citrate, pH 5, 5% (v/v) Triton-X 100] was added for 2 hours at 37°C in humidified atmosphere. Reaction was stopped with 5 mM EDTA/50 mM glycine (pH 10.4). Resulting chromophore was measured spectrophotometrically at 405 nm.

Cell function

Cell secretion of fibronectin and collagen I was determined by western blot. Passage 3 cells were seeded onto 60-mm dishes at a density of 1×10^5 cells per dish in the DMEM containing 10% FCS in the absence (control) or presence of 10 ng/mL bFGF and 1 mg/mL bFGF-loaded

NPs (dex-GMA/gelatin hydrogel NPs, equal to 10 ng/mL bFGF) at 37°C in humidified air containing 5% CO₂. The cells were harvested after 7 days. Cell lysates were prepared by adding 1 mL boiling lysis buffer (1% SDS), 1 mM sodium ortho-vanadate, and 10 mM Tris (pH 7.4) to BMSCs pellets. The protein concentration was quantitated with the BCA protein quantitation kit (Pierce Biotechnology, Rockford, IL, USA). Sixty micrograms of total cell lysate was electrophoresed on 12% for collagen I or 15% for fibronectin. Protein was isolated by SDS-PAGE electrophoresis, transferred onto polyvinylidene difluoride (Bio-Rad Laboratories, Hercules, CA, USA) by the semidry electrophoretic transfer technique, blocked with 5% skimmed milk and incubated with semidry electrophoretic transfer technique, blocked with 5% skimmed milk and incubated with polyclonal antibody against collagen I (SantaCruz, CA, USA) or a monoclonal antibody against fibronectin (Sigma) overnight at 4°C, and then incubated with the corresponding second antibody at room temperature for 1 hour after washing the membranes. An immunodetection kit was used for fluorescence detection (Pierce).

Statistical analysis

All quantitative data were expressed as the mean \pm SD. Nonparametric one-way analysis of variance and multiple comparisons were used to test for the assays of multiple comparisons to compare with the control by Software (SPSS 11.0). For the cell growth assay, a parametric analysis of variance based on the Turkey test was used. All assays were performed thrice, and a value of $P < 0.05$ was considered to be statistically significant.

Results and discussion

Synthesis of dex-GMA/gelatin hydrogel NPs

The amount of hydroxyl groups per dextran glucose ring substituted by GMA was estimated by the published ¹H-NMR method²⁵. There is an anomeric proton attached to the C1 position of dextran glucose ring and appears at 4.5–5.5 ppm in NMR spectrum, where the protons of hydroxyl groups appear. This proton does not react during the GMA substitution reaction, whereas some of the other protons of other hydroxyl groups are substituted by GMA. So the ratio of the normalized integrated intensities of the sum of the hydroxyl group peaks to the normalized integrated intensities of the anomeric proton peak, which can be used to estimate the DS. For un-substituted pure dextran, the ratio should be 3; whereas after substitution by GMA, this ratio should be more than 3. Thus, the DS could be calculated from the following ratio: 3 (difference of the NMR proton intensity

between dextran and dextran derivatives)/dextran. We have prepared two types of dex-GMA having DS 4.3% and 6.7%. It was found that the solubility of dex-GMA was greatly improved even with very low DS.

Gelatin and dextran are a pair of protein-polysaccharide, which can form IPNs from dex-GMA cross-linked in the presence of gelatin^{14,19}. Materials formed from IPNs share properties characteristic of each network. Enzymatically degradable IPNs from proteins and polysaccharides have been previously prepared. Both dextran and gelatin have great potential as biomaterials alone, but combining their properties can form hydrogel that may be selectively enzymatically degradable but not hydrolytically degradable. The drug delivery systems would selectively deliver their contents only at sites where appropriate biological enzymes are present and not simply in solution. Furthermore, gelatin would improve the biocompatibility when used in vivo. Chemical cross-linking of gelatin is accomplished traditionally with dilute solutions of glutaraldehyde or formaldehyde, but these cross-linking agents have been shown to be toxic. So in this study, thermal hardening with 1% glycer-aldehyde was performed on the NPs.

Characterization of NPs

Nanoparticle size

The NPs prepared in the discontinuous phase have a particle size of 320 ± 20 nm, and the DS of dex-GMA has no significant impact on particle size distribution. Figure 1 shows the size distribution of NPs prepared in this process. Almost all NPs had sizes ranging from 260 to 380 nm in diameter, and about 89.2% of the NPs were in an even narrower size range of 280–340 nm, and the results were 10–60 μ m, 60%, 20–40 μ m, respectively, in our previous studies¹³.

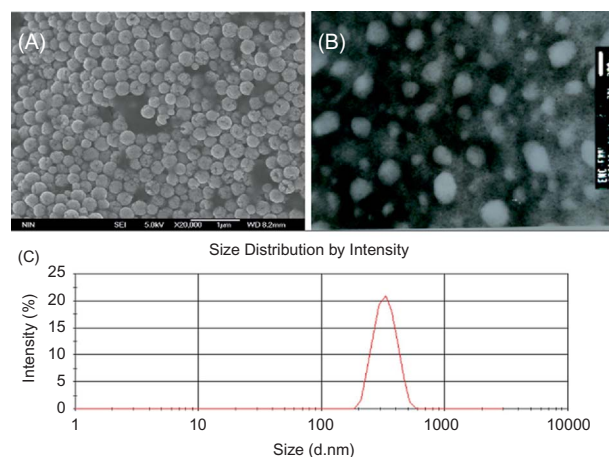


Figure 1. (A) Scanning electron micrograph, $\times 20,000$; (B) transmission electron micrograph, $\times 30,000$; (C) size distribution of dex-GMA/gelatin hydrogel nanoparticles.

Swelling and degradation

When dex-GMA/gelatin hydrogel NPs were incubated in the presence of dextranases (10 U/mL) at pH 7.4, a total degradation quickly occurred, and the degradation was evaluated. As a result, those hydrogel NPs were degraded between 20 and 40 days according to the DS of dex-GMA and the concentration of gelatin in PBS at 37°C in the presence of approximately 3 ng/mL dextranase.

Figure 2A shows the swelling behavior of dex-GMA/gelatin hydrogel NPs when incubated in 10 mM PBS at pH 7.4. The hydrogel NPs showed a progressive swelling in time, which was followed by a dissolution phase (in case of DS 6.7, a longer period was needed for complete dissolution). Figure 2B shows the dependence of maximum SRs at 37°C on the concentration of gelatin for hydrogel NPs. Within our prediction, the maximum SR of dex-GMA/gelatin hydrogel NPs decreased with an increase of the concentration of gelatin. Gelatin concentration of 5% had the highest SR, whereas the concentration of 2% was in the middle and the concentration of 0.2% obtained the smallest SR. On the other hand, as shown in Figure 3A, the DS of dex-GMA significantly influenced the swelling behavior of dex-GMA/gelatin hydrogel NPs. As a result, DS 4.3 and gelatin concentration of 5% gained the highest SR ($45.1 \pm 3.5\%$). The mass loss of dex-GMA/gelatin hydrogel NPs was also determined. As shown in Figure 2C, mass remaining value of hydrogel NPs obtained from dex-GMA with DS 4.3 remained below the type of dex-GMA with DS 6.7. By the end of day 20, these hydrogel NPs were completely degraded. Hydrogel NPs obtained from dex-GMA DS 6.7 exhibited slower degradation rates. So the conclusion can be drawn that the degradation of those hydrogel NPs was mainly influenced by the concentration of gelatin and DS of dex-GMA. This indicated that the hydrolysis of dex-GMA/gelatin hydrogel NPs would occur through a bulk erosion mechanism: A similar mechanism of hydrolysis was observed for poly(glycolic acid)/poly(lactic acid) polymers and poly(propylene fumarate-co-ethylene glycol) hydrogels^{17,23}. All hydrogels had very high water content [defined as $(SR - 1)/SR$] exceeding 97%, thereby facilitating the exchange of small hydrophilic molecules and nutrients between the hydrogel NPs and the cells.

It was well known that the swelling ability of hydrogel NPs was an important factor in regulating many of their properties, such as permeability to hydrophilic or hydrophobic drugs, biocompatibility, rates of enzymatic or hydrolytic degradation, and mechanical characteristics^{15,16}. The presence of chemically or enzymatically degradable bonds, that is, glucosidic linkages and ester groups, in the dex-GMA/gelatin hydrogel NPs conferred a potential biodegradability to these systems. This result suggested

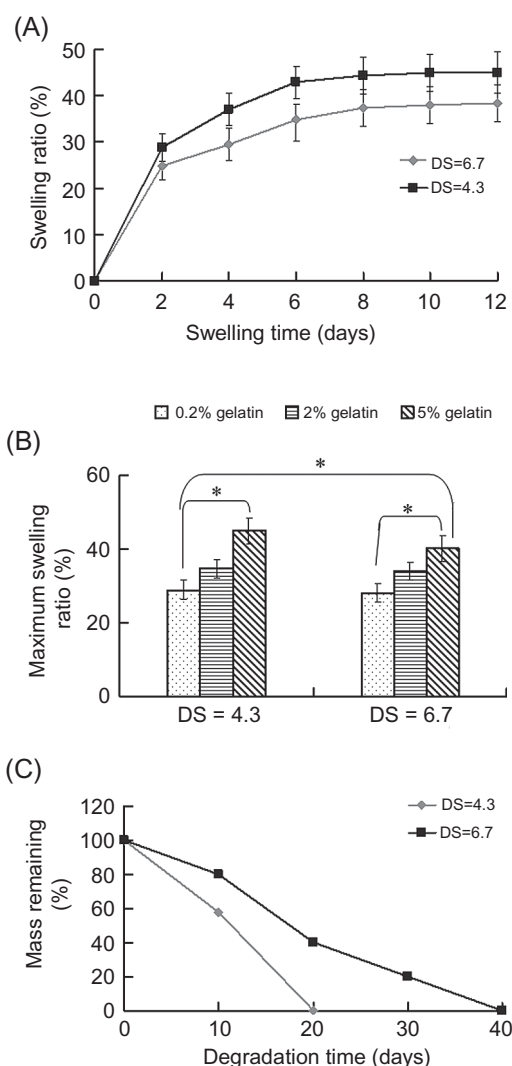


Figure 2. Swelling and degradation properties of dex-GMA/gelatin hydrogel nanoparticles obtained from different DS of dex-GMA (DS 4.3 and 6.7) and different concentration of gelatin in the polymerizing solution (pH 7.4, 37°C). (A) swelling ratio (SR) of dex-GMA/gelatin hydrogel nanoparticles (20 wt.% dex-GMA; 5 wt.% gelatin) as a function of time when immersed in 10 mM PBS. (B) Maximum swelling of dex-GMA/gelatin hydrogel nanoparticles (concentration of gelatin equals 5%, 2%, and 0.2%) when immersed in 10 mM PBS, * $P < 0.05$. (C) Mass remaining (%) during degradation of dex-GMA/gelatin hydrogel nanoparticles (20 wt.% dex-GMA; 5 wt.% gelatin) when immersed in 10 mM MPBS with the presence of dextranase (2 ng/mL). Data are shown as mean \pm SD ($n = 6$).

that dextran chains be still available to enzymatic hydrolysis by dextranases even after derivatization with GMA residues and further cross-linking.

Entrapment efficiency of dex-GMA/gelatin hydrogel NPs

bFGF could be encapsulated in the NPs with a very high efficiency. When bFGF was added to the phase-separated system, the encapsulation efficiency was $89.6 \pm 0.9\%$

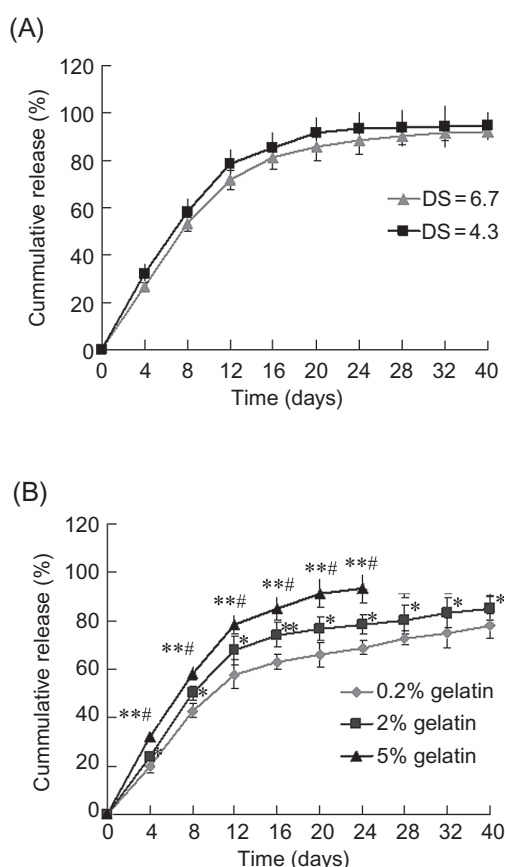


Figure 3. In vitro release of bFGF in PBS. (A) Profile of bFGF release from hydrogel nanoparticles with different DS. The values represent the mean \pm SD ($n = 6$). There was no significant difference between the durations of bFGF release from hydrogel nanoparticles with high and low DS of dex-GMA. (B) Cumulative release of bFGF from hydrogel nanoparticles prepared with different concentration of gelatin in the presence of dextranase. * $P < 0.05$, ** $P < 0.01$, significant differences of 5% gelatin group compared with 0.2% gelatin groups and 2% gelatin group compared with 0.2% gelatin groups at the same time-point. # $P < 0.05$, significant difference of 5% gelatin group was compared with 2% gelatin groups ($P > 0.05$). The values represent the mean \pm SD ($n = 6$).

(mean \pm SD). For five independently prepared nanoparticle batches, the bFGF-loaded % was $1 \times 10^{-3}\%$. After stored at 4°C in gelsiccation for about 6 months, the size of dex-GMA/gelatin NPs ranged from 290 to 390 nm in diameter, and the entrapment efficiency was also as high as $85.6 \pm 1.9\%$.

In vitro release of bFGF in PBS

The release of bFGF from the dex-GMA/gelatin hydrogel NPs studied was diffusion controlled. The apparent release rate was calculated from Higuchi plots. The release rate of bFGF from the dex-GMA/gelatin hydrogel NPs was affected by both the degree of GMA substitution of the dextran used and the concentration of gelatin. The effect of the degree of GMA substitution of the dextran on the release rate of bFGF was studied.

Figure 3A shows the release rate from dex-GMA/gelatin hydrogel NPs containing 5% (w/w) gelatin and 20% (w/w) glycidyl dex-GMA. Both NPs exhibited similar bFGF release profiles in standard PBS. No obvious burst release values from NPs under different DS (4.3 and 6.7) were found (Table 1). Both NPs exhibited a phase 1 release rate of approximately 5.8% per day from days 1–12 and a phase 2 release rate of approximately 0.8% per day from days 12–40. Accordingly, in vitro release of bFGF showed that the release was faster in the presence of dextranase in PBS than the absence of dextranase ($P < 0.05$). The release profiles of bFGF from NPs as a function of time showed that bFGF-releasing kinetics in vitro fitted to zero-order and Higuchi equations. The release profile in vitro was in accord with the two-phase kinetics law and more than 70% drug were released during 12 days. Furthermore, changing the DS of dex-GMA might influence bFGF release (Figure 3A). As the DS increased, the release rate at 37°C decreased. Figure 3B shows the effect of the gelatin concentration on the bFGF release rate from the hydrogel NPs containing 20% (w/w) dex-GMA with 4.3 substitution. The results showed that the release profiles were significantly different between the NPs with different concentration of gelatin. The release rate increased as the gelatin concentration increased at 37°C . The bFGF release duration from NPs could be varied from 24 to 40 days in accordance with different concentration of gelatin. These indicate that the release of the dex-GMA/gelatin hydrogel NPs be markedly affected by the gelatin concentration. These results suggest that we could obtain hydrogel NPs with an appropriate release profile by adjusting the degree of GMA substitution and the gelatin concentration. This might have important clinical meanings. In tissue or bone defect or tissue engineering, the need for concentration and interval of bFGF may be different^{15,16,18,19,21}. NPs could meet different demands of tissue regeneration, even at high concentration, could provide rapid release by decreasing the DS of dex-GMA and increasing the gelatin concentration,

Table 1. Phase 1 and 2 release rates and final cumulative bFGF release from nanoparticles in buffers of PBS and PBS with dextranase.

	Nanoparticles (DS of dex-GMA)	Buffer	
		PBS with dextranase	PBS
Phase 1 release rates (% day) (days 1–12)	4.3	5.8 ± 0.4	4.2 ± 0.4
	6.7	$6.6 \pm 0.5^*$	$5.1 \pm 0.5^*$
Phase 2 release rates (% day) (days 12–40)	4.3	0.8 ± 0.2	0.9 ± 0.1
	6.7	$1.4 \pm 0.2^*$	$0.36 \pm 0.1^*$
Final cumulative release (%)	4.3	92.1 ± 1.8	77.5 ± 2.1
	6.7	$85.3 \pm 2.3^*$	$70.3 \pm 3.1^*$

Reported significances (* $P < 0.05$) for the respective parameters result from comparing nanoparticles synthesized by different DS of dex-GMA in each buffer.

and promote secondary release by decreasing the DS of dex-GMA and increasing the gelatin concentration. The functionary mechanism needs to be studied further.

Bioactivity of bFGF-loaded dex-GMA/gelatin hydrogel NPs

Characteristics of BMSCs in culture

The MSCs attached on culture dishes sparsely, and the majority of the cells displayed a spindle-like shape. Mouse surface marker for MSCs has yet to be identified. The putative MSCs used in the experiments expressed CD29, CD44, and CD90 at moderate to high levels by flow cytometry analyses. The cells were negative for CD45 (a surface marker for hematopoietic stem cells) (Figure 4).

Mouse BMSCs cultured with bFGF NPs

BMSCs cultured with bFGF NPs or bFGF were in shuttle or spindle-like shape and formed 'hill and valley'

characteristic at confluence in 8 days. But when cells were incubated in the culture medium in the absence of bFGF, the cells became decrepit, with multiple interconnected umbos in different sizes and much granule-like substances in the surface of cells.

Proliferation assay of cell

To examine the cytotoxicity of the NPs and the biological activity of released bFGF, a cell proliferation assay was performed by BMSCs. BMSCs were incubated in the culture medium in the presence or absence of 10 ng/mL bFGF and 1 mg/mL bFGF-loaded NPs (dex-GMA/gelatin hydrogel NPs, equal to 10 ng/mL bFGF). Significant differences were found between the control group and the bFGF or bFGF-NPs group in 2 days ($P < 0.05$), but there were no statistical differences between bFGF and bFGF-NPs group ($P > 0.05$). After 6 days, the difference became significant between bFGF and bFGF-NPs group ($P < 0.05$) and more significant after 8 days ($P < 0.01$) (Figure 5A). This finding implies that these NPs can be useful as protein carriers without any significant

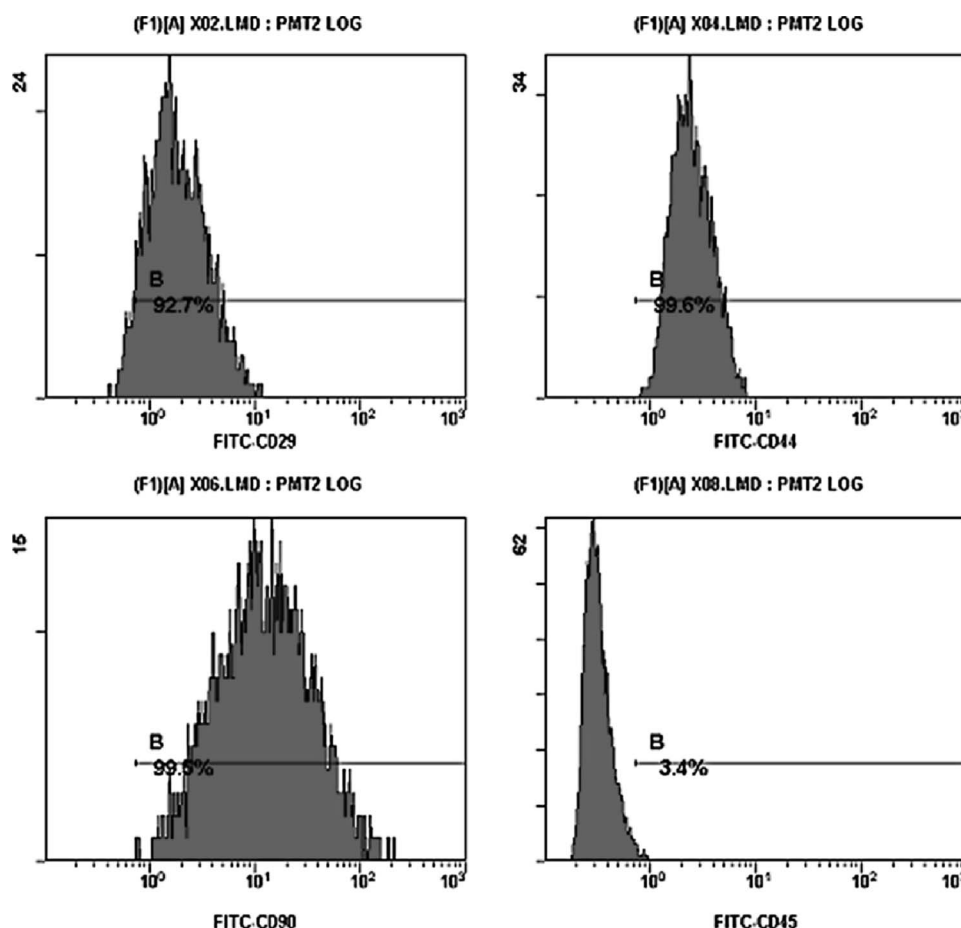


Figure 4. The bone marrow mesenchymal stem cells were determined by fluorescence-activating cell-sorting analysis (CD29, CD44, CD90, and CD45).

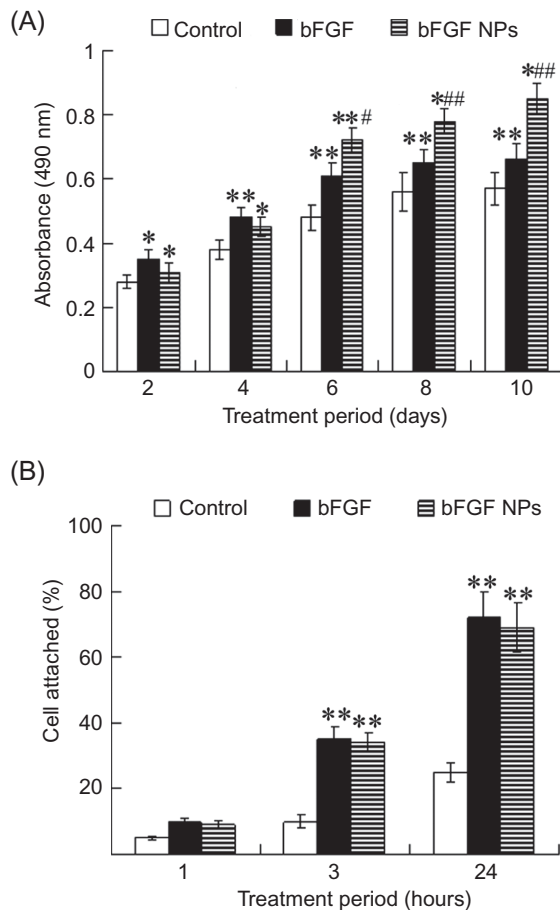


Figure 5. Effects of bFGF nanoparticles on cell metabolism (MTT assay) and cell attachment in mouse bone marrow mesenchymal stem cells. (A) MTT assay was used to determine the effects of bFGF nanoparticles on the metabolism of bone marrow stem cells. Cells were cultured in different culture for 2, 3, 5, 7, and 10 days in the presence (bFGF or bFGF NPs) or absence of 10 ng/mL bFGF (values are expressed as mean \pm SD, $n = 6$). * $P < 0.05$, ** $P < 0.01$, significant differences of control group were compared with bFGF groups or bFGF-NPs groups at the same time point. # $P < 0.05$, ## $P < 0.01$, significant differences of bFGF group were compared with bFGF-NPS group. (B) The attachment of bone marrow stem cells were observed after culture in different cultures for 1, 3, 24 hours in the presence (bFGF or bFGF-NPs) or absence of 10 ng/mL bFGF (values are expressed as mean \pm SD, $n = 6$). * $P < 0.05$, ** $P < 0.01$, significant differences of control group were compared with bFGF groups or bFGF-NPs groups at the same time point.

cytotoxic effects and can protect the bioactivity of loaded proteins.

Attachment assay

To observe the attachment ability of MSCs in different culture media, we carried out the attachment assay. Significant differences were found between control group and bFGF or bFGF-NPs group after 3 hours ($P < 0.05$), but there were no statistical

differences between bFGF and bFGF-NPs group ($P > 0.05$) (Figure 5B).

Changes in collagen I and fibronectin expression in the PBMCs

Collagen I and fibronectin expression were determined to observe the function of MSCs in different culture media. Figure 6A shows the representative western blot of collagen I and fibronectin expression of BMSCs cultured with different culture media 7 days later. Significant differences were found between control group and bFGF or bFGF-NPs group, and between bFGF and bFGF-NPs group ($P < 0.05$ or < 0.01) (Figure 6B and C). Collagen I and fibronectin expression were the highest in BMSCs cultured in PDGF-NPs group.

MSCs are nonhematopoietic multipotent stem cells that could differentiate into cells, such as cardiomyocytes and fibroblast, and also hard tissue cells, such as osteoblast and cementoblast, under the proper conditions in vitro and in vivo²⁶⁻²⁸. MSCs play a key role for some tissue regeneration. Furthermore, considering their advantages, such as the ease of obtaining bone marrow aspiration by a simple routine and the ability to self-renew, MSCs have been considered to be the ideal seeded cells for stem cells transplantation therapy research and tissue engineering^{27,28}. So, in our study, we chose MSCs as the experimental model in vitro.

Growth factor played a very important role in proliferation, secretion, attachment, mitogen, and

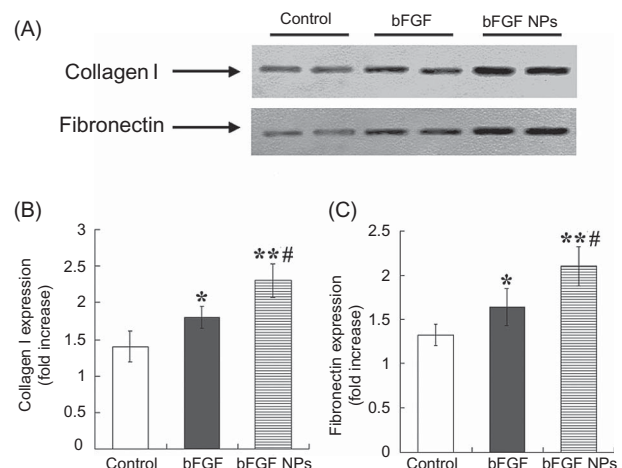


Figure 6. (A) Effects of bFGF nanoparticles on cell function (western blot) in mouse bone marrow mesenchymal stem cells after culture in different culture for 7 days in the presence (bFGF or bFGF NPs) or absence of 10 ng/mL bFGF (values are expressed as mean \pm SD, $n = 6$). (B) The representative western blot of collagen I and fibronectin expression of BMSCs cultured with different culture media 7 days later. (C) Significant differences were found between control group and bFGF or bFGF-NPs group and between bFGF and bFGF-NPs group ($P < 0.05$ or < 0.01).

differentiation for the stem cells. bFGF was reported to have a variety of biological activities²⁹ and to be effective in enhancing wound healing through induction of neovascularization³⁰ and regeneration of tissue³¹ and cartilage³² when administrated in the form of a solution. So we used bFGF as the experimental drug in this study.

Extracellular matrix secretion was regarded as one of the most important functions of cells. Cell proliferation, attachment, and differentiation, as well as the tissue regeneration all depend on the extracellular matrix secretion. Collagens are fibrous, extracellular matrix proteins with high tensile strength and are the major components of connective tissue, such as tendons and cartilage³³. Collagens also play a role in cell adhesion, which is important for maintaining normal tissue architecture and function, such as bone strength and platelet activation^{34,35}. Fibronectin is an extracellular matrix glycoprotein present on most cell surfaces, in extracellular fluids, and in plasma. It has been shown to be involved in various functions including cell adhesion, cell motility, and wound healing^{36,37}. According to these profiles and the outcome of our experiment, we hypothesized that more powerful secretion of FN and VN in bFGF NPs of MSCs would mainly be the cause of high adhesion rate in our research.

Conclusions

It was optimized that the novel method for preparing controlled size NPs by employing paraffin liquid (20 wt.% dex-GMA; DS 6.7%) and 5% gelatin and cross-linking with glyceraldehyde created IPNs with the most reproducible behavior. This strategy led to NPs of an average diameter of 320 nm (transmission electron microscope) from 250 to 380 nm and below encapsulating water-soluble polysaccharide and a stable long-term release of bFGF. Proliferation assay, attachment assay, and western blot showed that bFGF NPs had good biological effects on cultured BMSCs and could achieve a much longer action time than the same concentration of bFGF solution. Future work needs to be focused on optimizing the concentration of cross-linking agent or the duration of cross-linking to synthesize the therapeutically effective hydrogel NPs capable of surviving in the body for longer periods of time.

Acknowledgments

This study is supported by grants from the National Natural Science Foundation of China (No. 30600137), the National High Technology Research and Development Program of China (No. 2006AA02A138), and the

Science Foundation of healthy department of Shaanxi Province of China (No. 2006D45).

Declaration of interest: The authors report no conflict of interest. The authors alone are responsible for the content and writing of this article.

References

1. Harvey C. (2005). Wound healing. *Orthop Nurs*, 24:143–57.
2. Suh H. (2000). Tissue restoration, tissue engineering and regenerative medicine. *Yonsei Med J*, 41:681–4.
3. Kumar R, Dutt K. (2006). Enhanced neurotrophin synthesis and molecular differentiation in non-transformed human retinal progenitor cells cultured in a rotating bioreactor. *Tissue Eng*, 12:141–58.
4. Chayed S, Winnik FM. (2007). In vitro evaluation of the mucoadhesive properties of polysaccharide-based nanoparticulate oral drug delivery systems. *Eur J Pharm Biopharm*, 65:363–70.
5. Hussein MZ, Nasir NM, Yahaya AH. (2008). Controlled release compound based on metanilate-layered double hydroxide nanohybrid. *J Nanosci Nanotechnol*, 8:5921–8.
6. Kim SS, Min SP, Oju J, Cha YC, Kim BS. (2006). Poly(lactide-co-glycolide)/hydroxyapatite composite scaffolds for bone tissue engineering. *Biomaterials*, 27:1399–409.
7. Young S, Wong M, Tabata Y, Mikos AG. (2005). Gelatin as a delivery vehicle for the controlled release of bioactive molecules. *J Control Release*, 109:256–74.
8. Stenekes RJH, Loebis AE, Fernandes CM, Crommelin DJA, Hennink WE. (2001). Degradable dextran microspheres for the controlled release of liposomes. *Int J Pharm*, 214:17–20.
9. Kim IS, Jeong YI, Kim DH, Lee YH, Kim SH. (2001). Albumin release from biodegradable hydrogels composed of dextran and poly(ethylene glycol) macromer. *Arch Pharm Res*, 24:69–73.
10. van Dijk-Wolthuis WNE, Franssen O, Talsma H, van Steenberghe MJ, Kettenes-van den Bosch JJ, Hennink WE. (1995). Synthesis, characterization and polymerization of glycidyl methacrylate derivatized dextran. *Macromolecules*, 28:6317–22.
11. Cadée JA, de Groot CJ, Jiskoot W, den Otter W, Hennink WE. (2002). Release of recombinant human interleukin-2 from dextran-based hydrogels. *J Control Release*, 78:1–13.
12. Chen FM, Zhao YM, Wu H, Deng ZH, Wang QT, Zhou W, et al. (2006). Enhancement of periodontal tissue regeneration by locally controlled delivery of insulin-like growth factor-I from dextran-co-gelatin microspheres. *J Control Release*, 114:209–22.
13. Chen FM, Wu ZF, Sun HH, Wu H, Xin SN, Wang QT, et al. (2006). Release of bioactive BMP from dextran-derived microspheres: A novel delivery concept. *Int J Pharm*, 307:23–32.
14. Chen FM, Ma ZW, Dong GY, Wu ZF. (2009). Composite glycidyl methacrylated dextran (Dex-GMA)/gelatin nanoparticles for localized protein delivery. *Acta Pharmacol Sin*, 23:1–9.
15. Panyam J, Labhasetwar V. (2003). Biodegradable nanoparticles for drug and gene delivery to cells and tissue. *Adv Drug Deliv Rev*, 55:329–47.
16. Biondi M, Ungaro F, Quaglia F, Netti PA. (2008). Controlled drug delivery in tissue engineering. *Adv Drug Deliv Rev*, 60:229–42.
17. Mundargi RC, Babu VR, Rangaswamy V, Patel P, Aminabhavi TM. (2008). Nano/micro technologies for delivering macromolecular therapeutics using poly(D,L-lactide-co-glycolide) and its derivatives. *J Control Release*, 125:193–209.
18. Jabr-Milane L, van Vlerken L, Devalapally H, Shenoy D, Komareddy S, Bhavsar M. (2008). Multi-functional nanocarriers for targeted delivery of drugs and genes. *J Control Release*, 130:121–8.
19. Kosmala JD, Henthorn DB, Brannon-Peppas L. (2000). Preparation of interpenetrating networks of gelatin and dextran as degradable biomaterials. *Biomaterials*, 21:2019–23.

20. Tang MH, Dou HJ, Sun K. (2006). One-step synthesis of dextran-based stable nanoparticles assisted by self-assembly. *Polymer*, 47:728-34.
21. Zhang H, Gu CH, Wu H, Fan L, Li F, Yang F, et al. (2007). Immobilization of derivatized dextran nanoparticles on konjac glucomannan/chitosan film as a novel wound dressing. *Biofactores*, 30:227-40.
22. Yamamoto M, Ikada Y, Tabata Y. (2001). Controlled release of growth factors based on biodegradation of gelatin hydrogel. *J Biomater Sci Polym Ed*, 12:77-88.
23. Kopen C, Prockop DJ, Phinney DG. (1999). Marrow stromal cells migrates throughout forebrain and cerebellum, and they differentiate into astrocytes after injection into neonatal mouse brains. *Proc Natl Acad Sci USA*, 96:10711-6.
24. Landegren U. (1984). Measurement of cell numbers by means of the endogenous enzyme hexosaminidase. Applications to detection of lymphokines and cell surface antigens. *J Immunol Methods*, 67:379-88.
25. Kim SH, Chu CC. (2000). Synthesis and characterization of dextran methacrylate hydrogels and structural study by SEM. *J Biomed Mater Res*, 49:517-27.
26. Reilly GC, Radin S, Chen AT, Ducheyne P. (2007). Differential alkaline phosphatase responses of rat and human bone marrow derived mesenchymal stem cells to 45S5 bioactive glass. *Biomaterials*, 28:4091-7.
27. Makino S, Fukuda K, Miyoshi S, Konishi F, Kodama H, Pan J, et al. (1999). Cardiomyocytes can be generated from marrow stromal cells in vitro. *J Clin Invest*, 103:697-705.
28. Shi X, Sitharaman B, Pham QP, Liang F, Wu K, Edward Billups W, et al. (2007). Fabrication of porous ultra-short single-walled carbon nanotube nanocomposite scaffolds for bone tissue engineering. *Biomaterials*, 28:4078-90.
29. Gospodarowicz N. (1991). Biological activities of fibroblast growth factor. *Ann N Y Acad Sci*, 638:1-8.
30. McGee GS, Cavidson JM, Buckley A, Sommer A, Woodward SC, Aquino AM. (1988). Recombinant basic fibroblast growth factor accelerates wound healing. *J Surg Res*, 45:145-53.
31. Kawaguchi H, Kurokawa T, Hanada K, Hiyama Y, Tamura M, Ogata E. (1994). Stimulation of fracture repair by recombinant human basic fibroblast growth factor in normal and streptozotocin-diabetic rats. *Endocrinology*, 135:774-81.
32. Trippel SB. (1995). Growth factor actions on articular cartilage. *J Rheumatol Suppl*, 22:129-32.
33. Chan D, Lamande SR, Cole WG, Bateman JF. (1990). Regulation of procollagen synthesis and processing during ascorbate-induced extracellular matrix accumulation in vitro. *Biochem J*, 269:175-81.
34. McCarthy JB, Vachhani B, Iida J. (1996). Cell adhesion to collagenous matrices. *Biopolymers*, 40:371-81.
35. Eyre DR, Wu JJ, Fernandes RJ, Pietka TA, Weis MA. (2002). Recent developments in cartilage research: Matrix biology of the collagen II/IX/XI heterofibril network. *Biochem Soc Trans*, 30:893-9.
36. Nagai T, Yamakawa N, Aota S, Yamada SS, Akiyama SK, Olden K, et al. (1991). Monoclonal antibody characterization of two distant sites required for function of the central cell-binding domain of fibronectin in cell adhesion, cell migration, and matrix assembly. *J Cell Biol*, 114:1295-305.
37. Akiyama SK, Yamada KM, Hayashi M. (1981). The structure of fibronectin and its role in cellular adhesion. *J Supramol Struct Cell Biochem*, 16:345-8.